Dynamic Depolarized Light Scattering and Nuclear Magnetic Relaxation Studies of Isotactic Oligo- and Poly(methyl methacrylate)s in Dilute Solution

Yoshiharu Naito, Nobuo Sawatari, Yoshio Takaeda, Takenao Yoshizaki, and Hiromi Yamakawa*

Department of Polymer Chemistry, Kyoto University, Kyoto 606-01, Japan

Received November 12, 1996; Revised Manuscript Received February 7, 1997[⊗]

ABSTRACT: The (excess) power spectrum J_Γ of the depolarized component of scattered light intensity was measured for eight samples of isotactic oligo- and poly(methyl methacrylate)s (i-PMMA), each with the fraction of racemic diads $f_r \simeq 0.01$, in the range of weight-average degree of polymerization x_w from 4 to 70.1 in acetonitrile at 28.0 °C (Θ). The spin−lattice relaxation time T_1 was also determined for the three samples with $x_w = 4$, 5, and 70.1, and the nuclear Overhauser enhancement NOE, for the two samples with $x_w = 4$ and 70.1, all in acetonitrile at 35 °C. As in the cases of atactic (a-) polystyrene (a-PS) and a-PMMA previously studied, it is found that J_Γ may be well represented in terms of a single Lorentzian independently of x_w and that the relaxation time τ_Γ defined from J_Γ at infinite dilution increases with increasing x_w and levels off to its asymptotic value in the limit of $x_w \to \infty$, being consistent with the recent theoretical prediction on the basis of the helical wormlike (HW) chain model. A comparison is made of the present data for τ_Γ, T_1, and NOE with the HW theory, and it is shown that the theory may explain satisfactorily the data in the range of $x_w \gtrsim 10$, although semiquantitatively for τ_Γ. For $x_w \lesssim 10$, the rigid sphere model having the radius equal to the apparent root-mean-square radius of gyration of the HW chain may give a good explanation of τ_Γ but not of T_1, indicating that the dynamic depolarized light scattering and nuclear magnetic relaxation cannot be described in terms of a common single relaxation time. However, there is shown to be an effective (mean) magnetic relaxation time τ_M approximately equal to $0.6\tau_\Gamma$. From a comparison of the present results for τ_Γ for i-PMMA with the previous ones for a-PS and a-PMMA, it is shown that there is good correlation between the static and dynamic chain stiffness, the latter being defined as the ratio of the value of τ_Γ in the limit of $x_w \to \infty$ to that of the corresponding isolated repeat unit (monomer), as predicted by the HW theory.

Introduction

In previous papers,[1,2] an experimental study was made of local motions of (unperturbed) flexible polymer chains in dilute solution, carrying out dynamic depolarized light scattering (LS) and nuclear magnetic relaxation measurements on solutions of atactic polystyrene (a-PS)[1] and atactic poly(methyl methacrylate) (a-PMMA)[2] and their oligomers. The dynamical properties investigated were the spectrum J_Γ of the (excess) depolarized scattered component, the spin−lattice relaxation time T_1, and the nuclear Overhauser enhancement NOE, all of which may be expressed in terms of the same class of basic time-correlation functions within the framework of the dynamic theory[3] of the helical wormlike (HW) chain.[3,4] The conclusions obtained are summarized as follows. First, J_Γ of each test solution may be well represented in terms of a single Lorentzian, and for each polymer the relaxation time τ_Γ as defined as the reciprocal of the half-width at half-maximum (HWHM) of J_Γ increases with increasing molecular weight M and levels off to its asymptotic value in the limit of $M \to \infty$, the results being consistent with the HW theoretical prediction.[5] Second, T_1 and NOE are closely correlated with τ_Γ. Third, the dynamic HW theories[5−7] may explain semiquantitatively the dependences on M of these properties for $M \gtrsim 10^3$ except for NOE for a-PS, while the rigid sphere model with a single, proper relaxation time is valid for them for smaller M. Fourth, as far as the above two polymers are concerned, there is good correlation between dynamic and static chain stiffness, as predicted by the HW theory.[7]

In the present paper, we proceed to make a further study of these dynamical properties for isotactic (i-) PMMA in order to confirm the above conclusions. In particular, we examine the correlation between dynamic and static chain stiffness. The values of the static stiffness parameter λ^{-1} for i-PMMA,[8] a-PS,[9] and a-PMMA[10] determined from an analysis of their mean-square radius of gyration $\langle S^2 \rangle$ are 38.0, 20.6, and 57.9 Å, respectively. Thus the dynamic chain stiffness of i-PMMA may be expected to have a value intermediate between those for a-PS and a-PMMA.

As in the case of the previous study of a-PMMA,[2] we use acetonitrile as the Θ solvent for i-PMMA, the Θ temperature for this system being 28.0 °C.[8] The optical anisotropy of the solvent acetonitrile is larger than that of the solute i-PMMA[11] as in the case of a-PMMA,[12] so that the spectrum of the depolarized component obtained for the solution by the use of a Fabry−Perot (FP) interferometer should be properly decomposed into J_Γ and the contribution from the solvent. For this decomposition, we adopt the procedure already established in the study of a-PMMA.[2]

Experimental Section

Materials. All the i-PMMA samples used in this work are the same as those used in the previous studies of $\langle S^2 \rangle$, the intrinsic viscosity, the translational diffusion coefficient (in Θ and good solvents),[8,13−15] the scattering function,[16] the second virial coefficient,[17] and the mean-square optical anisotropy,[11] i.e., the fractions separated by preparative gel permeation chromatography (GPC) or fractional precipitation from the

[⊗] Abstract published in *Advance ACS Abstracts,* April 15, 1997.

S0024-9297(96)01668-3 CCC: $14.00

Table 1. Values of M_w, x_w, and M_w/M_n for Isotactic Oligo- and Poly(methyl methacrylate)s

sample	M_w	x_w	M_w/M_n
iOM4[a]	4.58×10^2	4	1.00
iOM5	5.58×10^2	5	1.00
iOM6	6.58×10^2	6	1.00
iOM7	7.89×10^2	7.31	1.01
iOM10[b]	1.01×10^3	9.52	1.02
iOM16	1.56×10^3	15.0	1.02
iOM31	3.12×10^3	30.6	1.04
iOM71	7.07×10^3	70.1	1.05

[a] M_w's of iOM4 through iOM7 had been determined from ^{1}H NMR and GPC.[8] [b] M_w's of iOM10 through iOM71 had been determined from LS in acetonitrile at 28.0 °C (Θ),[8,13] except for iOM16, whose M_w was determined from LS in acetone at 25.0 °C.[17]

original samples prepared by living anionic polymerization,[8] following the procedure of Ute et al.[18] They are sufficiently narrow in molecular weight distribution and have a fixed stereochemical composition (the fraction of racemic diads $f_r \simeq 0.01$) almost independent of the weight-average molecular weight M_w.[8] The values of M_w, the weight-average degree of polymerization x_w, and the ratio of M_w to the number-average molecular weight M_n are summarized in Table 1.

The solvent acetonitrile was purified according to a standard procedure prior to use.

Dynamic Depolarized Light Scattering. The photometer used for all dynamic depolarized LS measurements is the same as that used in the previous studies,[1,2,11,12] i.e., a Brookhaven Instruments Model BI-200SM goniometer with a minor modification of its light source part and with a detector alignment newly assembled to incorporate a Fabry−Perot (FP) interferometer in it. It has been described in detail in the previous paper,[12] and therefore we here only give its short sketch (see Figure 1 of ref 12).

Vertically polarized light of wavelength 488 nm from a Spectra-Physics Model 2020 argon ion laser equipped with a Model 583 temperature-stabilized etalon for single-frequency-mode operation was used as a light source. It was made highly vertically (v) polarized by passing through a Gran−Thompson (GT) prism with an extinction ratio smaller than 10^{-5}. The scattered light was measured at a scattering angle of 90°. Its horizontal (H) component, i.e., the depolarized (Hv) component, which was extracted from the total scattered light intensity by the use of the same GT prism as above, was analyzed with a Burleigh Instruments Model RC-110 FP interferometer equipped with a Model RC-670 pair of plane mirrors with a flatness of $\lambda/200$ and a reflectivity of 97.5%. The intensity of the Hv component filtered through the FP interferometer was measured by an EMI 9893B/350 photomultiplier (PM) tube. A pinhole of diameter 100 μm was used as a spatial filter, which was placed between the interferometer and the PM tube. All the measurements were carried out by the single passing, as in the previous studies.[1,2]

As before,[1,2] the transmittance $T(\omega)$ of the FP interferometer was determined by measuring the polarized component of the light intensity scattered from a solution of an a-PS sample with $M_w = 7.32 \times 10^5$ in methyl ethyl ketone at the concentration $c \simeq 1 \times 10^{-3}$ g/cm^3 and at 28.0 °C, following Ouano and Pecora.[19]

In the present study, the free spectral range (FSR) of the interferometer (i.e., the distance between the mirrors) was changed from 1.34×10^{11} to 1.07×10^{12} rad/s, depending on the width of J_Γ, in order to attain an appropriate resolution. As in the previous studies,[1,2] the value δ of FSR for each setting was determined by the use of the ^{4}He hyperfine structure interval of 1.0 cm^{-1} at 587.5 nm associated with the 2^3P-3^3D transition for $3 \times 10^{11} \lesssim \delta \lesssim 1.1 \times 10^{12}$ rad/s and of the Brillouin shift $\Delta\omega_B$ of 3.53×10^{10} rad/s in the Rayleigh−Brillouin spectrum of pure benzene at 25.0 °C at 1 atm for $10^{11} \lesssim \delta \lesssim 3 \times 10^{11}$ rad/s.

Measurements were carried out on solutions of all the samples in acetonitrile at 28.0 °C (Θ). The most concentrated solution of each sample in acetonitrile was prepared gravimetrically and made homogeneous by continuous stirring at ca. 35 °C for 1−2 days. This solution and the solvent were optically purified by filtration through a Teflon membrane of pore size 0.1 or 0.45 μm. The solutions of lower concentrations were obtained by successive dilution. The weight concentrations of the test solutions were converted to the solute mass concentrations c (in g/cm^3) by the use of the densities of the solutions.

Before and after each measurement on the solution or solvent, the transmittance of the FP interferometer was determined in the manner as described above. In the present measurements, the finesse could be kept at 30−60 during a single measurement, which took ca. 40 min.

Nuclear Magnetic Relaxation. T_1 of ^{13}C was determined for aliphatic carbon atoms of the samples iOM4, iOM5, and iOM71 by the inversion-recovery method with a pulse sequence $\pi-t-\pi/2$ on a JEOL JNM GX-400 spectrometer at 100.4 MHz. NOE for each of those carbon atoms of the samples iOM4 and iOM71 was evaluated from the ratio of the integrated intensity of its peak obtained with complete noise decoupling of protons to that obtained with gated decoupling only during data acquisition. A pulse delay was taken to be longer than 5 times as long as the largest T_1 of aliphatic carbon atoms under observation. Measurements were carried out on solutions in acetonitrile at 35 °C with a lock signal obtained from an external C_6D_{12} tube. The solutions were not degassed since T_1's of interest rarely exceeded 2 s, as shown later.

Results

Relaxation Time τ_Γ. As mentioned in the Introduction, we first extracted the desired spectrum J_Γ from a spectrum observed for each test solution by the use of the FP interferometer following the procedure described in the previous study.[2] We here reproduce only its essential points. The observed (apparent) spectrum may be represented by a convolution integral of the transmittance of the FP interferometer and the true spectrum, the latter being composed of J_Γ and the spectrum due to the optically anisotropic solvent acetonitrile. Assuming that J_Γ may be represented by a linear combination of several (practically six) Lorentzians and using the transmittance and the spectrum of the pure solvent experimentally determined, the coefficient (weight) and the HWHM of each Lorentzian may be determined by numerical deconvolution.

As in the cases of a-PS[1] and a-PMMA,[2] the HWHMs of the six Lorentzians so determined for each test solution were found to be the same, indicating that J_Γ may be fitted by a single Lorentzian. We then determine the (apparent) relaxation time τ_Γ as defined as the reciprocal of the HWHM of J_Γ thus determined, which is just the HWHM of the single Lorentzian in the present case. Figure 1 shows plots of τ_Γ against c for all i-PMMA samples in acetonitrile at 28.0 °C. Each plot follows a straight line and the value of τ_Γ at infinite dilution may be evaluated from its intercept.

The values of τ_Γ thus determined at infinite dilution are given in Table 2 along with those of $k_BT\tau_\Gamma/\eta_0$ with k_B the Boltzmann constant, T the absolute temperature, and η_0 the solvent viscosity. The latter values have been calculated from the former with the value 0.331 cP of η_0 for acetonitrile at 28.0 °C. As discussed in the previous papers,[1,2] the reduced relaxation time $k_BT\tau_\Gamma/\eta_0$ must be independent of solvent condition if the motions of the small molecules or the motional units in the polymer chain may be described in the diffusion limit and if the local chain conformation does not depend on that condition. In the previous study of a-PMMA,[2] the values of $k_BT\tau_\Gamma/\eta_0$ for methyl isobutyrate (MIB), the monomer of PMMA, in acetonitrile at 44.0 °C and in

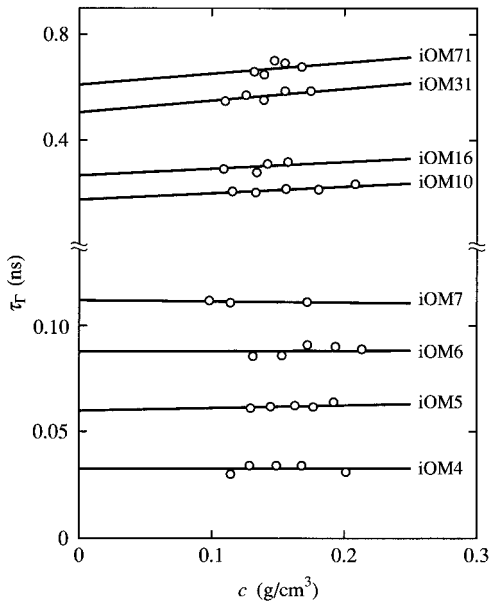

Figure 1. Plots of τ_Γ against c for all i-PMMA samples in acetonitrile at 28.0 °C.

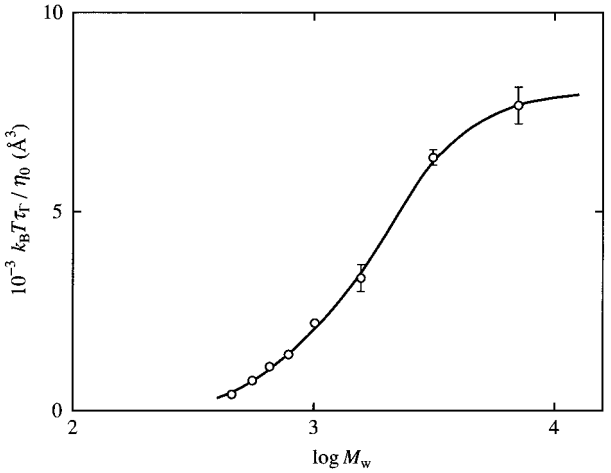

Figure 2. Plots of $k_BT\tau_\Gamma/\eta_0$ at infinite dilution against the logarithm of M_w for i-PMMA in acetonitrile at 28.0 °C. The solid curve connects the data points smoothly.

Table 2. Values of τ_Γ and $k_BT\tau_\Gamma/\eta_0$ for Isotactic Oligo- and Poly(methyl methacrylate)s in Acetonitrile at 28.0 °C at Infinite Dilution

sample	τ_Γ, ns	$k_BT\tau_\Gamma/\eta_0$, Å^3
iOM4	0.032_5	$4.0_8 \times 10^2$
iOM5	0.059_9	$7.5_3 \times 10^2$
iOM6	0.087_8	$1.1_0 \times 10^3$
iOM7	0.11_2	$1.4_1 \times 10^3$
iOM10	0.17_5	$2.2_0 \times 10^3$
iOM16	0.26_5	$3.3_3 \times 10^3$
iOM31	0.50_6	$6.3_6 \times 10^3$
iOM71	0.61_0	$7.6_6 \times 10^3$

carbon tetrachloride at 25.0 °C were found to agree well with each other, leading to the conclusion that the dynamics that governs τ_Γ may be described in the diffusion limit for solutions of a-PMMA in acetonitrile. This conclusion may be regarded as valid also for i-PMMA.

Figure 2 shows plots of $k_BT\tau_\Gamma/\eta_0$ at infinite dilution against the logarithm of M_w for i-PMMA in acetonitrile at 28.0 °C. The solid curve connects the data points smoothly. (The vertical line segments attached to the data points indicate the limits of experimental error.) As in the cases of a-PS[1] and a-PMMA,[2] the reduced relaxation time $k_BT\tau_\Gamma/\eta_0$ increases with increasing M_w and seems to level off in the limit of $M_w \to \infty$, the result being consistent with the HW theory.[5] Its asymptotic value in this limit is found to be ca. 8×10^3 Å^3, which is appreciably smaller than the corresponding value 2×10^4 Å^3 for a-PMMA[2] and larger than the value 4×10^3 Å^3 for a-PS.[1]

Table 3. Values of T_1 and NOE for iOM4 in Acetonitrile at 35 °C

$$\overset{1}{C}(CH_3)_3\overset{2}{C}H_2CCH_3(X)\overset{3}{C}H_2CCH_3(X)\overset{4}{C}H_2CCH_3(X)CH_2CCH_3(X)H$$

(X = $COOCH_3$)

carbon atom no.	T_1, s		NOE
	$c = 0.078$ g/cm^3	$c = 0.135$ g/cm^3	$c = 0.108$ g/cm^3
1	1.15	1.02	2.8_6
2	1.00	0.90	2.9_0
3	0.92	0.86	3.0_8
4	0.99	0.85	2.9_2

Spin−Lattice Relaxation Time T_1 and Nuclear Overhauser Enhancement NOE. As in the case of a-PMMA,[2] the methylene ^{13}C atoms in the main chain were observed. The values of T_1 and NOE for the sample iOM4 in acetonitrile at 35 °C are given in Table 3. As explicitly shown in its caption, the methylene carbon atoms have been numbered from the one in the initiating-end monomer group to the one in the terminating-end monomer group. In the previous case of the tetramer of a-PMMA having hydrogen atoms at both ends of the chain,[2] there are the four stereoisomers (or triads) labeled by *mm*, *mr*, *rm*, and *rr* with *m* and *r* indicating meso and racemic diads, respectively, and therefore four resonance peaks associated with these four stereoisomers were observed for each methylene carbon atom. (We note that the intensities of the peaks associated with the stereoisomer *mm* were very weak, and therefore their T_1 were not evaluated.) In contrast to that case, for the tetramer of i-PMMA having a *tert*-butyl group at the initiating end and a hydrogen atom at the other end,[8] there are in principle eight stereoisomers (or tetrads) and eight resonance peaks for each methylene carbon atom. However, seven peaks other than the one associated with the stereoisomer *mmm* are negligibly small, so that we only consider the latter one. We have identified each peak of the ^{13}C NMR spectra on the basis of the spectra obtained by Ute et al.[20] Thus the results in Table 3 are those associated with the stereoisomer *mmm*. We note that although we could not estimate experimental errors in the raw data, the errors in the evaluation of T_1 from the spectra are at most ca. ±2%. It is seen that the values of NOE obtained for the sample iOM4 are ca. 3 for all the ^{13}C atoms, corresponding to the narrowing limit.

For the sample iOM5, there are in principle 16 stereoisomers. However, we only consider the peaks associated with the stereoisomer *mmmm*, corresponding to the above case of iOM4. We have identified each peak of the methylene ^{13}C NMR spectra on the basis of the spectra obtained by Ute et al.[20] The results for their T_1 are given in Table 4. For the sample iOM71, we only consider the peak of the ^{13}C NMR spectra associated with the tetrad *mmm* by the use of the assignments determined by Ute et al.[20] The values of T_1 and NOE for the tetrad are given in Table 5.

As in the previous studies of a-PS[1] and a-PMMA,[2] we are interested in the motions of the center (or intermediate) part of the i-PMMA chain, so that we consider the value of T_1 averaged over the two values for the

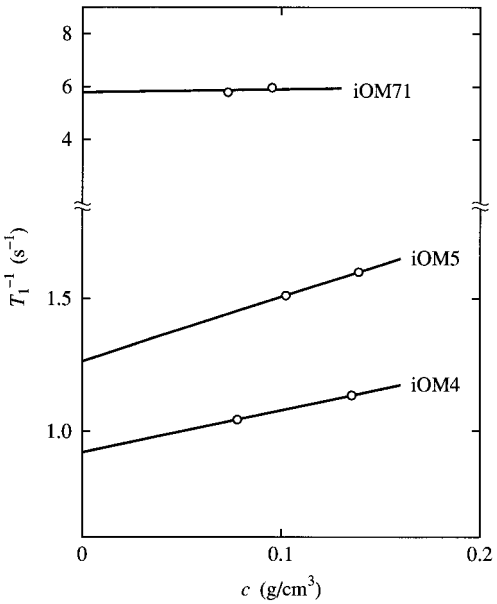

Figure 3. Plots of T_1^{-1} of ^{13}C against c for samples iOM4, iOM5, and iOM71 in acetonitrile at 35 °C.

Table 4. Values of T_1 for iOM5 in Acetonitrile at 35 °C

$C(CH_3)_3\overset{1}{C}H_2CCH_3(X)\overset{2}{C}H_2CCH_3(X)\overset{3}{C}H_2CCH_3(X)\overset{4}{C}H_2CCH_3(X)\overset{5}{C}H_2CCH_3(X)H$

(X = $COOCH_3$)

	T_1, s	
carbon atom no.	c = 0.102 g/cm^3	c = 0.139 g/cm^3
1	0.87_2	0.81_9
2	0.77_0	0.68_2
3	0.66_2	0.62_4
4	0.68_0	0.61_8
5	0.74_5	0.68_9

Table 5. Values of T_1 and NOE for iOM71 in Acetonitrile at 35 °C

c, g/cm^3	T_1, s	NOE
0.073	0.17_3	
0.095	0.16_8	
0.074		2.2_5

Table 6. Values of T_1 for Isotactic Oligo- and Poly(methyl methacrylate)s in Acetonitrile at 35 °C at Infinite Dilution

sample	T_1, s
iOM4	1.0_9
iOM5	0.79_1
iOM71	0.17_3

methylene ^{13}C atoms with $i = 2$ and 3 for iOM4 and the value of T_1 for $i = 3$ for iOM5. We note that for the sample iOM71 the results obtained are just those for the intermediate methylene ^{13}C atoms. Figure 3 shows plots of the reciprocal of the (mean) T_1 of the (center) ^{13}C atoms against c for the samples iOM4, iOM5, and iOM71. Extrapolation is made to infinite dilution from a pair of data at two concentrations for each sample, following the straight line indicated.

The values of T_1 thus evaluated at infinite dilution are summarized in Table 6. Note that for flexible polymer chains T_1 in general increases with decreasing relaxation time of the orientation of the C−H internuclear vector. It is seen that T_1 decreases with increasing M_w. Considering the previous results for a-PMMA,[2] the value 0.17 s for iOM71 may be regarded as the asymptotic value of T_1 in the limit of $M_w \rightarrow \infty$.

Discussion

HW Theory. Before proceeding to make a comparison of the present results of depolarized LS and nuclear magnetic relaxation measurements with the HW theory,[5−7] we briefly summarize its relevant results.

For the single (discrete) HW chain composed of N identical rigid subbodies, the power spectrum $J_\Gamma(\Delta\omega)$ of the depolarized component of the intensity scattered from it as a function of the difference $\Delta\omega$ between the angular frequencies of the scattered and incident light waves may be written in the form[5]

$$J_\Gamma(\Delta\omega) = \sum_{k\ \mathrm{odd}} \sum_{j=-2}^{2} A_k^j \frac{\tau_{2,k}^j}{1 + (\Delta\omega\tau_{2,k}^j)^2} \tag{1}$$

where

$$\tau_{2,k}^j = 1/\lambda_{2,k}^j \tag{2}$$

$$A_k^j = \frac{12\pi}{(N+1)} B_k^j \cot^2\left[\frac{\pi k}{2(N+1)}\right] \tag{3}$$

with

$$B_k^j = (8\pi^2)^{-1} \left| \sum_{j'=-2}^{2} \alpha_2^{j'} R_{2,k}^{jj'} \right|^2 \tag{4}$$

In eq 2, $\lambda_{2,k}^j$ are the eigenvalues of the matrix representation of the diffusion operator associated with the subspace (of full Hilbert space) spanned by the basis set with the "total angular momentum quantum number" $L = 2$ and the number of "excited" subbodies $n = 1$. Precisely, $J_\Gamma(\Delta\omega)$ is the Fourier−Laplace transform of a linear combination of the basic time-correlation functions associated with that subspace. We use the augmented eigenvalues $\lambda_{2,k}^j$ given by eq 25 of ref 7 (or eq 49 of ref 5) which takes partly into account the interactions with the complementary subspace. Thus $\lambda_{2,k}^j$ may readily be calculated for given values of N and six model parameters. They are the constant differential-geometrical curvature κ_0 and torsion τ_0 of the characteristic helix, the static stiffness parameter λ^{-1}, the bond length a, and the translational and rotatory friction coefficients ζ_t and ζ_r of the subbody. In eq 4, α_2^j are the spherical tensor components of the polarizability tensor affixed to the subbody, and $R_{2,k}^{jj'}$ is the transformation matrix associated with the eigenvalue problem of the above-mentioned matrix and is given by eq 40 of ref 5. We note that $R_{2,k}^{jj'}$ depends on the parameters κ_0, τ_0, and λ^{-1}. As explicitly shown in the previous theoretical paper,[5] Lorentzians only with very small k make a contribution to J_Γ because of the factor $\cot^2[...]$ involved in the amplitude A_k^j given by eq 3, and moreover, only those belonging to one or two branches (j) of the eigenvalue spectrum ($\lambda_{2,k}^j$) make a contribution because of the factor B_k^j given by eq 4. The resultant J_Γ may therefore be represented practically by a single Lorentzian. This is consistent with the previous and present experimental results.

We assume that the nuclear magnetic spin relaxes due to the heteronuclear dipolar interaction between two unlike spins I and S, with spin I observed and spin S irradiated and with the internuclear distance r

between them. Then T_1 and NOE for the above HW chain may be given by[6]

$$T_1^{-1} = (1/20)K^2 r^{-6}[J_0(\omega_S - \omega_I) + 3J_1(\omega_I) + 6J_2(\omega_S + \omega_I)] \quad (5)$$

$$\text{NOE} = 1 + \frac{\gamma_S}{\gamma_I}\left[\frac{6J_2(\omega_S + \omega_I) - J_0(\omega_S - \omega_I)}{J_0(\omega_S - \omega_I) + 3J_1(\omega_I) + 6J_2(\omega_S + \omega_I)}\right] \quad (6)$$

where

$$K = \hbar\gamma_I\gamma_S \quad (7)$$

$$J_m(\omega) = 2\sum_{k=1}^{N}(Q_{pk}^0)^2 \sum_{j=-2}^{2}\frac{A_{2,k}^j \tau_{2,k}^j}{1 + (\omega\,\tau_{2,k}^j)^2} \quad (8)$$

with

$$Q_{pk}^0 = [2/(N+1)]^{1/2} \sin[\pi pk/(N+1)] \quad (9)$$

and with $\tau_{2,k}^j$ and $A_{2,k}^j$ being given by eqs 2 and 26 of ref 6, respectively. In the above expressions, $\hbar$ is Dirac's constant (Planck's constant divided by 2π), γ_I and γ_S are the gyromagnetic ratios of spins I and S, respectively, and ω_I and ω_S are the respective Larmor angular frequencies. Note that I and S are ^{13}C and ^{1}H, respectively, in the present case, so that $I = S = {}^1/_2$. In eq 8, the index p indicates the subbody number.

Dependence of τ_Γ on x_w. Now we proceed to make a comparison of the present data for τ_Γ with the HW theory. Figure 4 shows plots of $k_B T\tau_\Gamma/\eta_0$ against the logarithm of x_w for i-PMMA in acetonitrile at 28.0 °C. The solid curve represents the HW theoretical values for τ_Γ as the reciprocal of the HWHM of J_Γ calculated from eqs 1−4 with the values of the (static) model parameters [$\lambda^{-1}\kappa_0 = 2.5$, $\lambda^{-1}\tau_0 = 1.3$, $\lambda^{-1} = 38.0$ Å, and $\lambda a = 0.081$ ($a = 3.07$ Å)],[8,21] those of the (dynamic) parameters [$r_1 \equiv \zeta_t/3\pi\eta_0 a = 1.0$ and $r_2 \equiv \zeta_r/a^2\zeta_t = 8.0$], and those of the Cartesian components of the polarizability tensor $\boldsymbol{\alpha}$ of the subbody given by[11]

$$\boldsymbol{\alpha} = \begin{pmatrix} 0.581 & \pm 0.266 & 0 \\ \pm 0.266 & 0.712 & 0 \\ 0 & 0 & -1.293 \end{pmatrix} \text{Å}^3 \text{ (i−PMMA)} \quad (10)$$

which is expressed in the localized coordinate system affixed to the subbody and is independent of the subbody number p. We note that the above value of λa has been evaluated from eq 22 of ref 21 with the value 0.0810 of $\lambda\Delta s = \lambda M_0/M_L$, where M_0 is the molecular weight of the repeat unit and is taken to be 100 for i-PMMA and M_L is the shift factor as defined as the molecular weight per unit contour length and has been determined to be 32.5 Å^{-1} for i-PMMA.[8] We also note that the above values of r_1 and r_2 are the same as those previously used for a-PMMA.[2] If we assume as in the previous studies[1,2] that the subbody is an oblate spheroid having the rotation axis of length a and the diameter d, then d is calculated to be 11 Å from eqs 35−38 of ref 22 with the above values of a, r_1, and r_2. This value of d is in rather good agreement with the value 9 Å previously[7] estimated from the chemical structure of i-PMMA, indicating that the values of r_1 and r_2 above are reasonable. We further note that the number N of subbodies in the chain has been set equal to x_w.

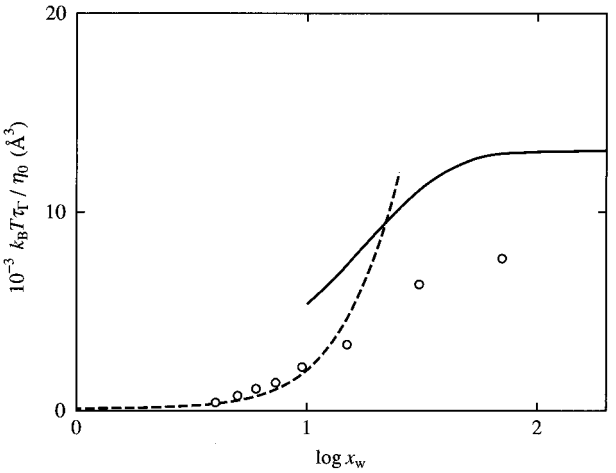

Figure 4. Plots of $k_B T\tau_\Gamma/\eta_0$ against the logarithm of x_w for i-PMMA in acetonitrile at 28.0 °C. The solid and dashed curves represent the theoretical values for the HW model and the rigid sphere model, respectively.

In Figure 4, we have omitted the HW theoretical values for $x_w \lesssim 10$ since the block-diagonal approximation[23] adopted in that theory breaks down in the range of such small N. The theoretical asymptotic value of $k_B T\tau_\Gamma/\eta_0$ in the limit of $x_w \to \infty$ is 1.31×10^4 Å^3 and is ca. 64% larger than the experimental value ca. 8.0×10^3 Å^3. As in the case of a-PMMA,[2] agreement between theory and experiment is only semiquantitative and is not so good as in the case of a-PS.[1]

As in the previous studies of a-PS[1] and a-PMMA,[2] we consider τ_Γ of the rigid sphere model having the radius equal to the apparent root-mean-square radius of gyration $\langle S^2\rangle_s^{1/2}$ of the HW chain and having a cylindrically symmetric polarizability tensor. It may be given by

$$\tau_\Gamma = 4\pi\eta_0\langle S^2\rangle_s^{3/2}/3k_B T \quad (11)$$

Recall that $\langle S^2\rangle_s$ is defined as the coefficient of the squared scattering vector k^2 in the expansion of the scattering function determined from small-angle X-ray scattering measurements and may be regarded as the mean-square radius of gyration of the excess electron density. Thus it may be given by

$$\langle S^2\rangle_s = \langle S^2\rangle + S_c^2 \quad (12)$$

where $\langle S^2\rangle$ is the (usual) mean-square radius of gyration of the HW chain contour of total length L and is given by eq 23 of ref 3 (or eq 24 of ref 2) and S_c is the (effective) radius of gyration of the cross section of the excess electron density distributed around the chain contour and has already been evaluated to be $\sqrt{8.2}$ Å for i-PMMA.[8] Values of τ_Γ calculated from eq 11 with eq 12 are represented by the dashed curve in Figure 4. We note that the contour length L of the HW chain has been converted to x_w by the use of the relation $x_w = M_L L/M_0$. The dashed curve may reproduce satisfactorily the data points for $x_w \lesssim 10$ as in the cases of a-PS and a-PMMA.

Dependences of T_1 and NOE on x_w. We make an analysis of the present results for T_1 and NOE along the same line as in the last subsection. Figure 5 shows plots of $n_{CH}T_1$ and NOE of the center methylene ^{13}C atoms against the logarithm of x_w for i-PMMA in acetonitrile at 35 °C, where n_{CH} is the number of C−H bonds attached to the ^{13}C atom under observation and is equal to 2 in the present case. The unfilled and

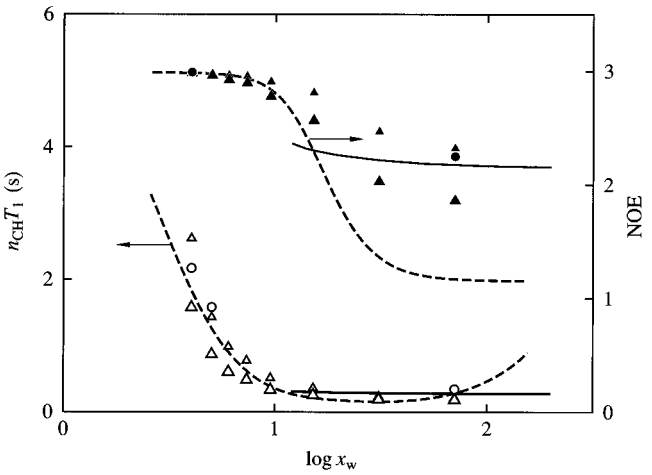

Figure 5. Plots of $n_{CH}T_1$ and NOE of ^{13}C against the logarithm of x_w for the center methylene carbon atoms for i-PMMA in acetonitrile at 35 °C (with $n_{CH} = 2$): (○) $n_{CH}T_1$; (●) NOE. The solid and dashed curves represent the theoretical values for the HW model and the rigid sphere model, respectively. The unfilled and filled large triangles represent the values of $n_{CH}T_1$ and NOE, respectively, calculated with $\tau_M = C\tau_\Gamma^*$ along with $C = 1$, and the small ones represent those with $C = 0.6$ (see the text).

filled circles represent the observed values of T_1 and NOE, respectively, and the solid curves represent the respective HW theoretical values calculated from eqs 5−9 with the same set of values of the static and dynamic model parameters as that used in the last subsection. For the calculation of the theoretical values of T_1 and NOE, we must specify the direction (α, β) of the C−H internuclear vector in the localized coordinate system, which is necessary for the calculation of the coefficients $A^j_{2,k}$ in eq 8. The values 90° and ±55° have been adopted as before[6] for the angles α and β in eq 26 of ref 6, respectively. We note that the coefficients $A^j_{2,k}$ in eq 8 and therefore J_m given by eq 8 do not depend on the sign of β when $\alpha = 90°$. This means that the two protons of the two bonded hydrogen atoms make equivalent contributions to T_1, and then T_1 calculated from eqs 5−9 with $\beta = 55°$ is just twice the observed T_1 and therefore corresponds to the observed $n_{CH}T_1$. For the Larmor angular frequencies ω_I and ω_S, we have used the values $2\pi \times 100.4 \times 10^6$ and $2\pi \times 399.2 \times 10^6$ rad/s, respectively, corresponding to the present measurements. Further, we have adopted the value 1.09 Å of r and the value 0.310 cP of η_0 for acetonitrile at 35 °C. The calculation of the theoretical values has been limited again to the range of N ($=x_w$) $\gtrsim 10$. For such large N, the values of T_1 and NOE observed for the center (intermediate) methylene carbon atoms are actually the mean values averaged over the position of ^{13}C, as noted above, so that we have presented the theoretical values averaged over p, which may be obtained by replacing $(Q^0_{pk})^2$ by N^{-1} in eq 8.

The HW theoretical values of both $n_{CH}T_1$ and NOE are almost independent of x_w (for $x_w \gtrsim 10$). Their asymptotic values in the limit of $x_w \to \infty$ are 0.276 s and 2.16, respectively, which are in rather good agreement with the values 0.34_6 s and 2.2_5, respectively, observed for the sample iOM71. The agreement between the theoretical and experimental values of T_1 is somewhat poorer than in the case of a-PMMA.[2] However, as in that case, the agreement between those of NOE is fairly good, in contrast to the case of a-PS.[1]

As in the case of J_Γ, we next consider the rigid sphere model having the radius $\langle S^2\rangle_s^{1/2}$, to which a C−H internuclear vector is affixed. T_1 and NOE may then be given by eqs 5 and 6, respectively, with J_m given by[24]

$$J_m(\omega) = \frac{2\tau_M}{1 + (\omega\tau_M)^2} \tag{13}$$

where τ_M is identical with τ_Γ given by eq 11. Note that T_1 thus obtained corresponds to the observed $n_{CH}T_1$, as in the case of the HW theoretical values above. In Figure 5, values of $n_{CH}T_1$ and NOE thus calculated from eqs 5 and 6, respectively, with eq 13 and with the above values of ω_I, ω_S, r, and η_0 are represented by the respective dashed curves. Roughly, the dashed curve for T_1 may explain semiquantitatively the data points for the samples iOM4 and iOM5 as well as for τ_Γ. Precisely, however, the differences between the observed and calculated values of T_1 for them are not very small as in the case of a-PMMA. This disagreement implies that T_1 cannot be explained in terms of the single relaxation time τ_Γ for i-PMMA as well as for a-PMMA (with a given M_w) in contrast to the case of a-PS, although this is possible for J_Γ for all of them.

As before,[1,2] we then examine values of T_1 and NOE calculated from eqs 5 and 6 with eq 13, where we equate τ_M to the scaled τ_Γ in acetonitrile at 35 °C, which we denote by τ_Γ^*, taking account of the differences in η_0 and T by the use of the equation

$$\tau_\Gamma^* = [(\eta_0/T)_{35}/(\eta_0/T)_{28.0}]\tau_\Gamma \tag{14}$$

with the *observed* values of τ_Γ in acetonitrile at 28.0 °C. If T_1 and NOE could be explained in terms of this τ_Γ^*, their calculated values would agree well with the observed ones. Values of $n_{CH}T_1$ and NOE thus calculated for all the samples are represented by the unfilled and filled large triangles, respectively, in Figure 5. For the sample iOM71, the calculated value of NOE is appreciably smaller than the observed one.

As previously mentioned,[2] the above discrepancy may be regarded as arising from the differences in relative weights (A^j_k in eq 1 and $A^j_{2,k}$ in eq 8) of the eigenvalues $\lambda^j_{2,k}$ between J_Γ given by eq 1 and J_m given by eq 8 and also those among a-PS and a- and i-PMMAs. Thus we simply relate an *effective* mean (single) magnetic relaxation time τ_M to τ_Γ^* by

$$\tau_M = C\tau_\Gamma^* \tag{15}$$

as before,[2] where C is a constant independent of M chosen so that values of T_1 and NOE calculated from eqs 5 and 6, respectively, with eqs 13−15 (and with the observed τ_Γ) are close to the observed ones. In Figure 5, the unfilled and filled small triangles represent the values thus calculated with $C = 0.6$, which happens to be the same as that previously used for a-PMMA.[2] As in that case, these calculated values agree well with the observed ones except for T_1 at large x_w, for which the former values are still ca. 40% smaller than the latter. As for a-PS, we note that $C \simeq 1$ (as previously found) and then that the corresponding calculated values of T_1 at large x_w are ca. 30% smaller than the observed ones.

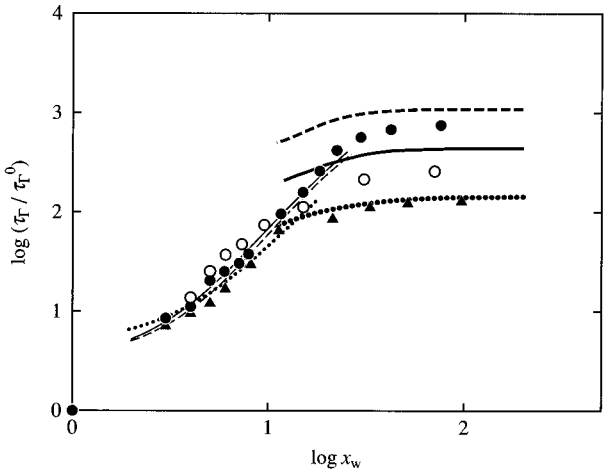

Figure 6. Double-logarithmic plots of $\tau_\Gamma/\tau_\Gamma^0$ against x_w, where τ_Γ^0 is the τ_Γ of the isolated monomer: (○) present data for i-PMMA in acetonitrile at 28.0 °C; (●) previous data for a-PMMA in acetonitrile at 44.0 °C;[2] (▲) previous data for a-PS in cyclohexane at 34.5 °C.[1] The heavy solid, dashed, and dotted curves represent the respective HW theoretical values, and the light curves represent the respective values for the rigid sphere model.

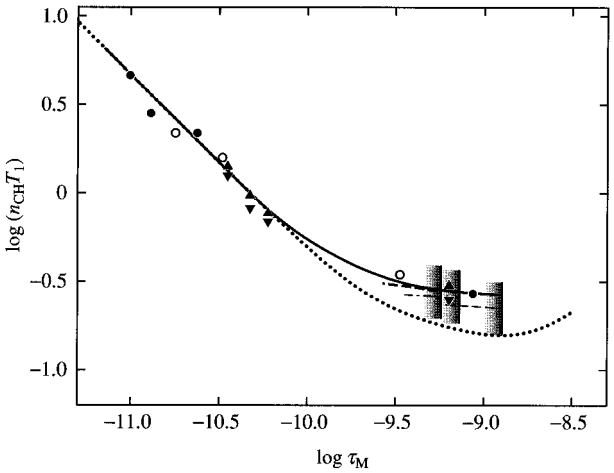

Figure 7. Double-logarithmic plots of $n_{CH}T_1$ (in s) against τ_M (in s): (○) present data for the center methylene ^{13}C atoms for i-PMMA in acetonitrile at 35 °C (with $n_{CH} = 2$); (●) previous data for the center methylene ^{13}C atoms for a-PMMA in acetonitrile at 44 °C (with $n_{CH} = 2$);[2] (▲) previous data for the center methylene ^{13}C atoms for a-PS in cyclohexane at 40 °C (with $n_{CH} = 2$);[1] (▼) previous data for the center methine ^{13}C atoms for a-PS in cyclohexane at 40 °C (with $n_{CH} = 1$).[1] The heavy and light dashed curves represent the HW theoretical values for i- and a-PMMAs, respectively, the dot-dashed curve represents those for a-PS, the dotted curve represents the values for the rigid sphere model, and the solid curve connects the data points smoothly (see the text).

Comparison with a-PMMA and a-PS. Finally, in this subsection we compare the present results for i-PMMA with the previous ones for a-PMMA[2] and a-PS.[1] Figure 6 shows double-logarithmic plots of $\tau_\Gamma/\tau_\Gamma^0$ against x_w for i-PMMA in acetonitrile at 28.0 °C (Θ) (unfilled circles), a-PMMA in acetonitrile at 44.0 °C (Θ) (filled circles), and a-PS in cyclohexane at 34.5 °C (Θ) (filled triangles), where τ_Γ^0 is the τ_Γ of the monomer (isolated repeat unit), i.e., $\tau_\Gamma^0 = 0.0023_6$ and 0.0019_3 ns for PMMA (MIB) in acetonitrile at 28.0 and 44.0 °C, respectively,[2] and $\tau_\Gamma^0 = 0.0056_2$ ns for a-PS (cumene).[1] The value 0.0023_6 ns of τ_Γ^0 in acetonitrile at 28.0 °C has been evaluated from the value 0.0019_3 previously[2] determined in acetonitrile at 44.0 °C by assuming that the reduced relaxation time $k_BT\tau_\Gamma^0/\eta_0$ is independent of T. We note that the values of the reduced relaxation time $k_BT\tau_\Gamma^0/\eta_0$ are $29._6$ and $31._1$ Å^3 for MIB and cumene, respectively, and are in good agreement with each other. The asymptotic value $\tau_{\Gamma,\infty}/\tau_\Gamma^0$ of the ratio $\tau_\Gamma/\tau_\Gamma^0$ in the limit of $x_w \rightarrow \infty$ represents the degree of restriction on the rotational motion of the isolated motional unit (monomer) due to its incorporation into the long enough polymer chain and may be regarded as a measure of "dynamic chain stiffness" (concerning J_Γ), as discussed in the previous theoretical study.[7] The heavy solid, dashed, and dotted curves represent the HW theoretical values of τ_Γ for i- and a-PMMAs and a-PS, respectively, divided by the respective observed ones of τ_Γ^0, and the light curves represent the respective values for the rigid sphere model.

Although the values of the ratio $\tau_\Gamma/\tau_\Gamma^0$ for i- and a-PMMAs and a-PS are close to each other in the oligomer region with very small x_w, they deviate from each other with increasing x_w. In the limit of $x_w \rightarrow \infty$, the value of the ratio for i-PMMA is intermediate between those for a-PMMA and a-PS, as was expected. Considering the fact that the HW theoretical values have been calculated by the use of the values of the model parameters determined from the equilibrium properties along with the proper values of the dynamic parameters, it may be concluded that the dynamic HW theory may explain well the difference in $\tau_{\Gamma,\infty}/\tau_\Gamma^0$ among i- and a-PMMAs and a-PS, although agreement between theory and experiment for the former two is only semiquantitative.

In order to examine the relation between T_1 and τ_M, values of $n_{CH}T_1$ (in s) are double-logarithmically plotted against τ_M (in s) in Figure 7 for the center methylene ^{13}C atoms for i-PMMA in acetonitrile at 35 °C (unfilled circles), a-PMMA in acetonitrile at 44 °C (filled circles), and a-PS in cyclohexane at 40 °C (filled triangles) and for the center methine ^{13}C atoms for a-PS in cyclohexane at 40 °C (filled, inverted triangles), where values of τ_M have been calculated from eq 15 with the values of τ_Γ^* and τ_Γ for i- and a-PMMAs, respectively, both with $C = 0.6$, and with the value of τ_Γ^* (at 40 °C) for a-PS with $C = 1$. Although the values of T_1 for the methylene ^{13}C atoms for a-PS at infinite dilution were not evaluated in the previous paper,[1] we evaluated them in the same manner as mentioned in the Results.[2] Further, for a-PS (in cyclohexane at 40 °C), we have used the values of the scaled τ_Γ (i.e., τ_Γ^*) evaluated in the previous paper.[1] The heavy and light dashed curves represent the HW theoretical values calculated for i- and a-PMMAs, respectively, in the same manner as in the previous subsection, and the dot-dashed curve represents those for a-PS. The right-end point of each curve bounded by the vertical line segment with the shade corresponds to the asymptotic value of τ_Γ in the limit of $x_w \rightarrow \infty$, and the other end point corresponds to $x_w = 10$. The dotted curve represents the values calculated from eq 5 with eq 13 for the rigid sphere model. Note that in the figure the data for both the center methylene and methine ^{13}C atoms for a-PS have been plotted in order to show explicitly the difference in T_1 between them mentioned in the previous paper.[1] However, this difference is seen to be rather small, and therefore we ignore it here. It is seen that the data points for i- and a-PMMAs and a-PS form nearly a single-composite curve, as shown by the solid curve, and follow the dotted curve for small τ_M (for $\log n_{CH}T_1 \gtrsim -0.2$), as was expected.

Conclusion

The power spectra J_Γ of the excess depolarized component of the light intensity scattered from i-PMMA in acetonitrile at 28.0 °C (Θ) have been accurately determined by following the data-processing procedure previously developed in order to extract J_Γ from observed spectra including the contribution of the optically anisotropic solvent. Then it has been found that J_Γ may be well represented in terms of a single Lorentzian independently of x_w and that the relaxation time τ_Γ defined from J_Γ increases with increasing x_w and levels off to its asymptotic value in the limit of $x_w \rightarrow \infty$, as in the cases of a-PS[1] and a-PMMA[2] previously studied, being consistent with the recent theoretical prediction on the basis of the HW chain model.[5] Precisely, the HW theory may explain semiquantitatively the observed dependence of τ_Γ (or J_Γ) on x_w over that range of x_w for which the theory is applicable, i.e., for $x_w \gtrsim 10$, while the rigid sphere model,[1,2] having the radius equal to the apparent root-mean-square radius of gyration $\langle S^2 \rangle_s^{1/2}$ of the HW chain, may reproduce well the data for $x_w \lesssim 10$. From a comparison of the present results for i-PMMA with the previous ones for a-PMMA and a-PS, it is shown that there is good correlation between the dynamic chain stiffness, as previously defined as the ratio of the relaxation time associated with the local motion of a long polymer chain to that of its isolated repeat unit (monomer), and the static chain stiffness λ^{-1}, as predicted by the HW theory.

As for the results of nuclear magnetic relaxation measurements, the HW theory can explain them quantitatively for T_1 and also for NOE for sufficiently large x_w. As in the case of a-PMMA, the rigid sphere model fails to give a quantitative explanation of T_1 even for $x_w \lesssim 10$, indicating that the dynamic depolarized scattering and nuclear magnetic relaxation cannot be described in terms of a common single relaxation time, but there is an effective (mean) magnetic relaxation time τ_M approximately equal to $0.6\tau_\Gamma$.

References and Notes

(1) Takaeda, Y.; Yoshizaki, T.; Yamakawa, H. *Macromolecules* **1994**, *27*, 4248.
(2) Takaeda, Y.; Yoshizaki, T.; Yamakawa, H. *Macromolecules* **1995**, *28*, 682.
(3) Yamakawa, H. In *Molecular Conformation and Dynamics of Macromolecules in Condensed Systems*; Nagasawa, M., Ed.; Elsevier: Amsterdam, 1988; p 21.
(4) Yamakawa, H. *Annu. Rev. Phys. Chem.* **1984**, *35*, 23.
(5) Yoshizaki, T.; Yamakawa, H. *J. Chem. Phys.* **1993**, *99*, 9145.
(6) Yamakawa, H.; Fujii, M. *J. Chem. Phys.* **1984**, *81*, 997.
(7) Yamakawa, H.; Yoshizaki, T.; Fujii, M. *J. Chem. Phys.* **1986**, *84*, 4693.
(8) Kamijo, M.; Sawatari, N.; Konishi, T.; Yoshizaki, T.; Yamakawa, H. *Macromolecules* **1994**, *27*, 5697.
(9) Abe, F.; Einaga, Y.; Yoshizaki, T.; Yamakawa, H. *Macromolecules* **1993**, *26*, 1884.
(10) Tamai, Y.; Konishi, T.; Einaga, Y.; Fujii, M.; Yamakawa, H. *Macromolecules* **1990**, *23*, 4067.
(11) Takaeda, Y.; Yoshizaki, T.; Yamakawa, H. *Macromolecules* **1995**, *28*, 4167.
(12) Takaeda, Y.; Yoshizaki, T.; Yamakawa, H. *Macromolecules* **1993**, *26*, 3742.
(13) Sawatari, N.; Konishi, T.; Yoshizaki, T.; Yamakawa, H. *Macromolecules* **1995**, *28*, 1089.
(14) Kamijo, M.; Abe, F.; Einaga, Y.; Yamakawa, H. *Macromolecules* **1995**, *28*, 1095.
(15) Arai, T.; Sawatari, N.; Yoshizaki, T.; Einaga, Y.; Yamakawa, H. *Macromolecules* **1996**, *29*, 2309.
(16) Horita, K.; Yoshizaki, T.; Hayashi, H.; Yamakawa, H. *Macromolecules* **1994**, *27*, 6492.
(17) Kamijo, M.; Abe, F.; Einaga, Y.; Yamakawa, H. *Macromolecules* **1995**, *28*, 4159.
(18) Ute, K.; Asada, T.; Miyatake, N.; Hatada, K. *Makromol. Chem., Macromol. Symp.* **1993**, *67*, 147.
(19) Ouano, A. C.; Pecora, R. *Macromolecules* **1980**, *13*, 1167.
(20) Ute, K.; Nishimura, T.; Hatada, K. *Polym. J.* **1989**, *21*, 1027.
(21) Yamakawa, H.; Yoshizaki, T. *J. Chem. Phys.* **1981**, *75*, 1016.
(22) Yoshizaki. T.; Yamakawa, H. *J. Chem. Phys.* **1984**, *81*, 982.
(23) Yamakawa, H.; Yoshizaki, T.; Shimada, J. *J. Chem. Phys.* **1983**, *78*, 560.
(24) Solomon, I. *Phys. Rev.* **1955**, *99*, 559.

MA961668U